Oct 18th, 12:00 AM

Behavior of Connections Between SHS Columns & W-section Beams

Uk Sun Kim

Jong Suk Lee

Young Bong Kwon

Twelfth International Specialty Conference on Cold-Formed Steel Structures
St. Louis, Missouri, U.S.A., October 18-19, 1994

Behavior of Connections between SHS Columns & W-Section Beams

Uk Sun Kim[1], Jong Suk Lee[2], Young Bong Kwon[3]

ABSTRACT

Connections between SHS (Square Hollow Section) columns and W-section beams are generally fabricated by welding with or without endplates in the factory. These welded connections possess some finite degree of rotational stiffness which falls between fully rigid and ideally pinned joints. The influence of partially restrained connections on structural response not only changes the moment distribution but also increases frame drift. In this paper, a series of connection tests joining SHS column and W-section beam were executed and the test results compared with theoretical values. A method to utilize nonlinear moment-rotation relations of beam-to-column connections in steel framed structures is proposed. For the problem of contact in endplate-type connections, a simple and efficient method is also introduced.

1) Research Institute of Industrial Science and Technology, Building and Construction Laboratory, KOREA
2) Ulsan University, Department of Civil Engineering, KOREA
3) YeungNam University, Department of Civil Engineering, KOREA

1. Introduction

Connections have a rotational stiffness which ideally falls between hinged beam-column joints and fully restrained joints. Over the past few decades, various kinds of connections of hot-rolled wide flange sections have been studied widely and AISC Specification ASD (1989), LRFD (1986), ECCS (1990) all have provisions for the semi-rigid connections of W-sections. Semi-rigid joints affect the moment distribution, horizontal frame drift and energy dissipation ability of steel framed structures. It has been found that in seismic regions semi-rigidity holds design benefits. While W-section columns are widely used in high-rise buildings, in Korea, built-up box columns have also been used for several high-rise buildings. The use of cold-formed square hollow sections as column members is on the increase due to the double symmetry of the sections which enable them to resist horizontal force in both-directions without braces for a multi-story building, in addition to low production costs. Apart from Japan, where three types of diaphragms are used to resist local failure at the flange of SHS sections and to fully ascertain rigidity, in non-seismic regions, the W-section beam can be directly welded to the SHS column with or without endplates, if semi-rigid connections are used for the design purpose. The behavior of connections between large SHS columns and W-sections has been studied by Morita (1990), and concrete filled SHS columns have been studied by Teraoka and Morita(1991).

In this paper, the connections between SHS columns and W-section beams are studied for application to multi-story buildings. Three connection types - directly welded(DW), welded with an endplate(EW), and welded with an endplate with additional plug welding(PW) - are tested. The test results are compared with numerical simulation results. A simple and efficient way for frame analysis , with consideration of the effects of semi-rigidity, is proposed. The nonlinear moment-rotation relation is also modelled for nonlinear analysis of steel frames.

2. Material Properties

Two cold-formed SHS columns and hot-rolled W-sections(which is called H-section in Korea and H-section will be used in this paper from here) selected for connection tests are SHS 400mm×400mm×12mm, SHS 400mm×400mm×16mm and H 300mm×200mm×8mm×12mm, H 400mm×300mm×10mm×16mm, nominal yield strength σ_y=240MPa(34.8ksi), these sections are designed for a six-story commercial building. Measured test section geometries and dimensions are given in Fig. 1 and Table 1. The SHS sections are formed without post-forming stress relief process which cause complex distribution of yield stress and residual stress around the section.

Table 1. Dimensions of test sections

(unit : mm)

Specimen	Columns (SHS)			Beams (H-section)			
	A	B	t	H	B	t_1	t_2
CON 1-1	350	350	9	250	200	9	9
CON 1-2	350	350	9	400	300	9	9
CON 1-3	350	350	15	250	200	9	9
CON 1-4	350	350	15	400	300	15	20
HDP 1-1	400	400	12	300	200	8	12
HDP 1-2	400	400	12	400	300	10	16
HDP 1-3	400	400	16	300	200	8	12
HDP 1-4	400	400	16	500	300	11	18

(1 in = 25.4mm)

2.1 General

The method of cold-forming, such as roll-forming, cause changes in the mechanical properties from the virgin steel of the sections. These changes generally include increases in yield and ultimate tensile strengths and reductions in ductility. Significant changes are normally induced in the corners of the sections as a result of plastic straining. The changes in the flat area of the sections are also significant comparing to the nominal strength. The stress-strain curve of the SHS sections shows usually gradual yielding as a result of the varying amount of plastic strain through rolling and cold-forming process. The percentage of increase in the ultimate strength is much smaller than that in yield strength for the corner areas.

2.2 Coupon tests

Tensile coupons were taken from the flat areas, corners and welded parts of the sections to investigate the effects of plastic strain and welding on the mechanical properties. The tensile coupons were prepared and tested according to Korean Standard KSB0801, KSB0802. The corner coupons had their ends flattened using a grinder and gripped in the same manner as flat tensile coupon. The tensile coupons were tested using an Instron Testing Machine Model 1127(250kN). A calibrated extensometer of 10mm gauge length was mounted on the edges of the coupons to measure the longitudinal strain.

The results of the flat and corner tensile coupon tests are summarised in Table 2. The 0.2% proof stress was used as the yield stress for the coupons since they all exhibited gradual yielding on the stress-strain curves. The static yield stresses of the coupons are obtained by stopping extension for one minute in the vicinity of yield. The mean difference between static and dynamic yield stress were negligible.

Table 2. Mechanical Properties of Materials Used

Location	Yield Strength MPa (ksi)	Tensile Strength MPa (ksi)	Elongation %
flat area	347.5 (50.4)	431.5 (62.6)	31.5
corner	484.5 (70.3)	537.5 (77.9)	-
welded part	435 (63.1)	502 (72.8)	20.4

The mean measured Young's Modulus (E) is 2.0 × 10^5 MPa and the mean yield stress of 350 MPa is higher than the minimum yield stress of SS41(σ_y=240MPa) steel specified in KS D3505. The mean measured ultimate strength(σ_u) was found to be 430 MPa. The yield stress of the corner areas was found to be 40% higher than the flat areas and the ultimate tensile stress was increased by 25% compared to the flat areas. The increases of welded areas is 16% in yield stress and 25% in ultimate stress. The elongation of the welded areas is decreased approximately 35% of that of the flat areas.

2.3 Residual Stress

In this investigation, longitudinal released surface strains, which were mainly caused by the cold-forming process, were measured using electrical resistance strain gauge and sectioning techniques. Due to the symmetry of the sections, the measurements were carried out on one quarter of the sections and several additional points as shown in Fig. 2. The section was sliced using a band-saw machine. To protect the strain gauges from damage, a thick layer of protection material was applied before sectioning. The commercially produced cold-formed square hollow sections tested had no post-forming stress relieving heat treatment. The resulting locked-in residual stress approaches the yield stress of the material and is distributed in a complex fashion around the section. The distribution of the residual stress is quite similar to the results of others(Weng and Pekoz, Key and Hancock). Consequently, tensile residual stress exists at the outside of the SHS column, while compressive residual stress exists at the inside of the SHS column, residual stress distribution on the SHS column which will be used in the beam-column connection tests is shown in Fig. 3.

3. Stub Column test

Two different size square hollow section, TS 1-1, TS 1-2 (SHS 200mm×200mm×6mm), TS 2-1, TS 2-2 (SHS 200mm×200mm×9mm)were tested as stub columns over a length not less than three times the section width, in accordance with the recommendations of Johnston(1976). This length was chosen to minimize the influence of end support conditions on local buckling at the same time precluding overall column buckling effects which may occur if a larger section were to be tested. The test results are given in Table 3. By comparison with the coupon test results, the maximum residual stress was found to be over 24% of the yield stress of the flat coupon for TS1 and 16% for TS2

TABLE 3. Results of stub column test

Specimen	P_y kN (kips)	P_{max} kN (kips)	σ_y MPa (ksi)	σ_{max} MPa (ksi)
TS 1-1	1200(264)	1700(374)	263(38.1)	372.6(54)
TS 1-2	1200(264)	1700(374)	263(38.1)	372.6(54)
TS 2-1	1900(418)	2800(616)	285(41.3)	420(60.9)
TS 2-2	2000(440)	2900(638)	300(43.5)	435(63.1)

4. Beam-column connection tests

4.1 General

The test section was in real size which could be commonly used in multi-story buildings. The connections were fabricated by welding. Three connection types tested were as follows;

1. DW-TYPE : H-section(W-Section in USA) was directly welded to the flange of the SHS column
2. EP-TYPE : H-section was welded to the SHS with endplate.
3. PW-TYPE : H-section was welded in the same manner as EP-TYPE with additional plug welding applied between column flange and endplate.

The section geometries and dimensions are given in Table 4 and Fig. 4.

Table 4. Dimension of connection test specimens

(unit : mm)

Specimen	Columns (SHS)			Beams (H-section)				Endplate			Weld throat
	A	B	t	H	B	t_1	t_2	A	B	t	size
DW 1	200	200	6	150	150	7	10	-	-	-	8
EP 1	200	200	6	150	150	7	10	175	200	9	8
HP 1	200	200	6	150	150	7	10	175	250	9	8
DW 2	400	400	12	294	200	8	12	-	-	-	8
EP 2	400	400	12	294	200	8	12	350	400	12	8
HP 2	400	400	12	294	200	8	12	350	400	12	8
DW 3	200	200	9	150	150	7	10	-	-	-	8
EP 3	200	200	9	150	150	7	10	160	345	9	8
HP 3	200	200	9	150	150	7	10	160	345	9	8

(1 in = 25.4mm)

The contact ends of the H-sections of 750mm length were end milled by an electronic milling machine and were welded at a right angle with special appliance at both flanges of the SHS column. The beams were simply supported at both ends to give straight line

between the end of the beam and the flange of the column, and the downward load was applied on the SHS column. The test configurations were given in Fig. 5. Since stiffness of the H-sections was enough to remain straight before the rotational angle of the flange of the SHS column approached 0.015 radian which was calculated from the deflection limit (ℓ/300, ℓ : span length) at the beam center for Korean Building Code. The rotational angle obtained from the beam rotation could be taken as the rotation of the flange of SHS column.

4.2 Test results

From the test readings, the rotation was calculated as Eq(4.1)

$$\theta_{avg} = \frac{\theta_1+\theta_2}{2} \tag{4.1}$$

where

$$\theta_1 = \frac{(d_2+d_5)-(d_1+d_6)}{350\times 2}, \quad \theta_2 = \frac{(d_3+d_4)-(d_1+d_6)}{650\times 2} \tag{4.2}$$

The connection tests were continued until cracks at welds were found and addition of load was impossible.

The moment at the flange of the SHS column was obtained from Eq(4.3)

$$M = \frac{P}{2} \cdot 700 \ (\mathrm{t}\cdot\mathrm{mm}) \tag{4.3}$$

The test results are given and also compared with the plastic moments of the H-beam in Table 5.

Table 5. Results of connection test

Specimen	P_y kN (kip)	P_{max} kN (kip)	M_y kN·m(ft-k)	M_{max} kN·m(ft-k)	$K_{\theta i}$ kN·m/rad(ft-k/rad)
DW 1	27.3(6)	31.8(7)	15(11)	17.5(12.9)	690 (507.4)
EP 1	50.9(11.2)	52.7(11.6)	28(20.6)	29(21.3)	965 (709.6)
HP 1	50.9(11.2)	52.7(11.6)	28(20.6)	29(21.3)	1300 (956)
DW 2	102(22.4)	204.4(25)	72(52.9)	143.1(105.2)	2790 (2051.5)
EP 2	157(34.6)	316(69.5)	110(80.9)	221.3(162.7)	6650 (4889.7)
HP 2	167(36.8)	312(68.6)	117(86)	218.2(160.4)	7660 (5632.4)
DW 3	41.8(9.2)	55.6(12.2)	23(16.9)	30.6(22.5)	780 (573.5)
EP 3	43.6(9.6)	64.5(14.2)	24(17.6)	35.5(26.1)	1060 (779.4)
HP 3	54.5(12)	83.4(18.3)	20(22.1)	46.4(34.1)	2100 (1544)

P_{max} and M_{max} indicates the ultimate loads and ultimate moments corresponding to the maximum value on the P-δ, M-θ graphs. P_y was determined by plotting the load against the square of lateral deflection and subsequently fitting a line through the test results in the post-yielding region. The intersection of the fitted line and load axis was assumed to be P_y. A second set of experimental yield loads were determined by examining the change in the slopes of the load-deflection curves. The change in overall stiffness was subtle in some

tests and so the choice of intersection was difficult. However, the average value of the two methods was taken as the experimental yield load. Initial rotational stiffness was calculated by Eq (4.4).

$$K_{\theta i} = \frac{M_i}{\theta_i} \tag{4.4}$$

The failure mode of the beam-column connection is shown in Fig. 6. Deformations occurred not only at the flange but at the web of the SHS columns in a manner similar to Zhao's (1991) test sections where tubular sections were welded to tubular sections.

5. Yield line method

The theoretical analysis of the plastic moment capacity of SHS column and H-section beam connections was carried out by Morita(1992). In this paper Morita equation is modified for DW type connections and extended to EP type conections. Yield line models assumed are shown in Figs. 7a and 7b.

The plastic moment equations for DW and EP type are given in Eq (5.1), (5.2), respectively.

$$M_{py} = h_b \cdot {}_nP_y \tag{5.1a}$$

$${}_nP_y = M_p \cdot b_c' \left[\frac{4x+h_b+r_t}{x^2} + \frac{2}{h_b-r_t} \right] + \frac{(M_a+M_p)}{M_p \cdot b_c'} \left[x - \frac{m \cdot M_p \cdot b_c'}{(m_a+M_p)x} \right]^2 t_b \cdot {}_b\sigma_y \tag{5.1b}$$

$$r_t = t_b + 2S \tag{5.1c}$$

$$b_c' = b_c - (4-1.5\sqrt{2}\,) \cdot t_c \tag{5.1d}$$

$${}_nP_y = \frac{P_t+P_c}{2}\ ,\ M_{py} = h_b \cdot {}_nP_y \tag{5.2a}$$

$$\begin{aligned} P_c =\ & 2(y-m) \cdot t_b \cdot {}_b\sigma_y - \frac{(y^2-m^2) \cdot t_b \cdot {}_b\sigma_y}{y} \\ & + \frac{2M_a \cdot x + 2M_a \cdot x_1 + 2M_a \cdot r_t + 2M_p \cdot r_t + 2M_{p1} \cdot x_1}{y} \\ & + \frac{M_{p1} \cdot b_c + M_p \cdot b_c - 2M_p \cdot y}{x} + \frac{M_p \cdot b_c - 2M_p \cdot y + 2M_{p1} \cdot y}{x_1} \\ & + \frac{2M_p \cdot k_1}{(y-k_2)} \cdot L_1 + \frac{2M_p \cdot (y-k_2)}{k_1} \cdot L_1 \\ & + \frac{2M_{p1} \cdot k_2}{(x-k_1)} \cdot L_2 + \frac{2M_{p1} \cdot (x-k_1)}{k_2} \cdot L_2 \end{aligned} \tag{5.2b}$$

$$P_t = 2(y-m)\cdot t_b \cdot {}_b\sigma_y - \frac{(y^2-m^2)\cdot t_b \cdot {}_b\sigma_y}{y} + \frac{2M_a\cdot x + 2M_a\cdot x_1 + 2M_a\cdot r_t + 2M_{ep}\cdot r_t + 2M_{p1}\cdot x_1}{y} + \frac{M_{p1}\cdot b_c + M_{ep}\cdot b_c - 2M_{ep}\cdot y}{x} + \frac{M_{ep}\cdot b_c - 2M_{ep}\cdot y + 2M_{p1}\cdot y}{x_1} + \frac{2M_{ep}\cdot k_1}{(y-k_2)}\cdot L_1 + \frac{2M_{ep}\cdot (y-k_2)}{k_1}\cdot L_1 + \frac{2M_{p1}\cdot k_2}{(x-k_1)}\cdot L_2 + \frac{2M_{p1}\cdot (x-k_1)}{k_2}\cdot L_2 \quad (5.2c)$$

$$M_a = \frac{{}_c\sigma_y \cdot {}_ct_w^2}{4}\ ,\ M_p = \frac{{}_c\sigma_y \cdot (ct_f + t_e)^2}{4}$$
$$M_{p1} = \frac{{}_c\sigma_y \cdot {}_ct_f^2}{4}\ ,\ M_{ep} = \frac{{}_c\sigma_y \cdot {}_ct_e^2}{4} \quad (5.2d)$$

Differently from Morita's assumption, corner areas were so difficult to have plastic hinge line that modified mechanism enabled to get closer values to the experimental results.

For the connections with an extended endplate, The distance(x) which is from the top flange of the H-beam to the end of the yield line should be calculated first and be compared with the extended length of the endplate(k_1).

The thickness applied should be decided as follows;

1. $k_1 < x$ $\quad t_c = t_{col} + t_{ep}$ or t_{col}
   $\quad t_t = t_{ep}$ or t_{col}
2. $k_1 \geq x$ $\quad t_c = t_{col} + t_{ep}$
   $\quad t_t = t_{ep}$

The details are given in Kim et al(1994). The theoretical results are compared with the test results obtained and are given in Table 6.

Table 6. Comparison with test results

Specimen	Test Results		Results of Analysis				M_{yt} / M_{yc}
	M_{yt} kN·m(ft-k)	M_{max} kN·m(ft-k)	M_{yc} kN·m(ft-k)	x mm	y mm	M_b kN·m(ft-k)	
DW 1	15(11)	17.5(12.9)	15.2(11.2)	52.9	29.7	72.6(53.4)	0.99
EP 1	28(20.6)	29(21.3)	28.8(21.2)	92.2	52.2	72.6(53.4)	0.97
DW 2	72(52.9)	143.1(105.2)	73.8(54.3)	142.3	107.3	251.2(184.7)	0.98
EP 2	110(80.9)	221.3(162.7)	102.8(75.6)	203.5	137.1	251.2(184.7)	1.07

The plastic moments of the H-beams and ultimate moments are also given in the Table 6 for comparison. The theoretical results are in good agreement with the experimental results. The ratios of experimental plastic moment to theoretical plastic moment range from 0.97 to 1.07. Since the formulae are based on the yield lines, the formulae may not produce reasonable values if the thickness of the SHS column is too thick to have clear yield line.

6. Structural Analysis for steel framed structures

6.1 Simulation of connections

The values of Young's Modulus and Poisson's ratio have been taken as 2.0×10^5 MPa(2.9×10^4ksi) and 0.3 respectively in the analysis. The stress-strain relation was assumed as bilinear (elastic-perfectly plastic) and yield stress has been taken as 340 MPa(49.3ksi).

The moment-rotation curves of the test connections is given in Fig. 8. Test results are compared with the theoretical behavior predicted by advanced analysis (plastic nonlinear analysis) using ABAQUS. The typical deformed mode of connection is given in Fig. 9. The thickness of the compression side has been taken as total thickness of the column and endplate and the tension side as thickness of the endplate for simplicity if endplate were attached. For more accurate simulation of the connection with endplates, interface element between flange of the column and endplate was assumed and the fillet welded line was assumed completetly connected. The results are compared with the test reslts and simple simulation in Fig. 10. The results obtained using interface elements are quite similar to the results with simple assumption. For the connections with plug welded endplate, differently from the expectation, the predicted behavior falls between results obtained with above mentioned assumption and results which were obtained with the assumption that the total thickness of column and endplate is effective.

6.2 Application of the rotational stiffness to the structural analysis

The joint rotational stiffness ($K_{\theta d}$) which was mentioned previous section could be applied for the first order analysis of a three story building. The axial rigidity EA of the connection elements was defined to be the same as that of H beam, but the rotational stiffness of the connection obtained was modelled by a beam of length of half of column width. The moment of inertia(I) should satisfy the condition.

$$K_{\theta d} = \frac{EI}{L} \tag{6.1}$$

In the analysis, instead of initial rotational stiffness of the connection, $K_{\theta 0.015}$ was used. $K_{\theta 0.015}$ was the secant stiffness corresponding to the rotation(θ = 0.015rad) which was obtained with the assumption that the deflection curve was parabola and the maximum allowable deflection at the center of the beam was $\ell/300$. The applied load was horizontal wind load and vertical load. The moment resultants are shown in Fig. 11a and the moment resultants of rigid framed structures are given in Fig. 11b for comparison.

From the results, due to the flexibility, the moment distribution is quite different. For the vertical loading only, semi-rigidity did not produce significantly unconservative stress. But for the horizontal force applied, the moments on the column of the semi-rigid frame is slightly higher than that of the rigid frame and the frame drift should be controlled for serviceability.

7. Conclusions

The use of large size square hollow sections was studied. Due to the flexibility of beam-column connections without diaphragm, design provisions for semi-rigid joints should be made for the construction of buildings. The theoretical plastic moment based on the yield line method produced quite reasonable values compared with the connection test. The first order analysis of a semi-rigid framed structure against horizontal force showed unconservative strength compared with the rigid frame. However, in practice, if we consider the diaphragm effect of floor slab and the potential ability of energy dissipation, semi-rigid connections can be applied to frame analysis.

8. Acknowledgement

The financial support of Pohang Iron & Steel Co. Ltd. and the donation of the test materials of Hyundai Pipe Co. Ltd. are gratefully acknowledged.

9. References

[1] American Institute of Steel Construction, Manual of Steel Construction (ASD) 9th ed., Chicago, IL, 1989.

[2] American Institute of Steel Construction, Load & Resistance Factor Design, Specification for Structural Steel Buildings, Chicago, IL, September 1986.

[3] European Convention for Constructional Steelwork (ECCS), Analysis and Design of Steel Frames with Semi-Rigid Joints, Document No. TWG 8.1/8.2, ECCS, Brussels, Belguim, 1990.

[4] Hibbit, Karlsson & Sorensen, Inc., ABAQUS User's Manual, Version 5.3, 1993.

[5] Johnston, B.G. (editor) Guide to Stability Design Criteria for Metal Structures, 3rd edn., Structural Stability Research Council, Wiley-Interscience, 1976.

[6] Key, P.W. and Hancock, G.J., "A Theoretical Investigation of the Column Behavior of the Cold-formed Square Hollow Sections" Research Report, No. R584, School of Civil and Mining Engineering, University of Sydney, Australia, 1981.

[7] Kim Uk Sun et al., "A Study on the Strength of H-Beam to SHS Column Connections Based on the Yield Line Theory", Vol. 10, No. 6, Journal of the Architectural Institute of Korea, June 1994.

[8] Koji Morita et al., "Analysis on the Strength of Unstiffened Beam Flange to RHS Column Connections Based on the Combined Yield Line Theory", E. Niemi, Tubular Structures -the Third International Symposium, ELSEVIER SCIENCE PUBLISHERS LTD., 1990.

[9] Koji Morita et al., "Experimental Study on Connections Between Concrete Filled Square Tubular High Strength(780 N/mm^2) Steel Column and H-Beam", Proceedings of the Third PSSC, JSSC, 1992.

[10] Korean Standard Association, Korean Industrial Standard B0801, B0802, D3505, 1992.

[11] Weng, C.C. & Pekoz, T., "Residual Stress in Cold-formed Steel Members", Journal of Structural Engineering, ASCE, 116(6), pp1611-1625.,1990.

[12] Zhao, X.L. & Hancock, G.J.,Plastic Mechanism Analysis of T-Joint in RHS Under Concentrated Force, Research Report NO. R644, The University of Sydney, School of Civil and Mining Engineering, 1991. 11

10. Notations

θ : Rotational angle (radian)
ν : Poisson's ratio
σ_y : Yield stress
σ_u : Ultimate stress
$d_1 \sim d_6$: Dial gauge reading
E : Young's Modulus
k : Extended length of endplate
$K_{\theta d}$: Design rotational stiffness
$K_{\theta i}$: Initial rotational stiffness
M : Moment
M_p : Plastic moment
P : Applied concentrated load
t_c, t_t : Thickness of compression and tension side respectively
t_{col} : Thickness of column
t_{ep} : Thickness of endplate

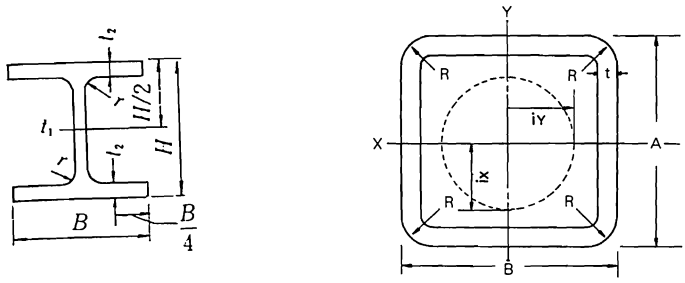

Fig. 1 Shape and Dimension of Test Sections

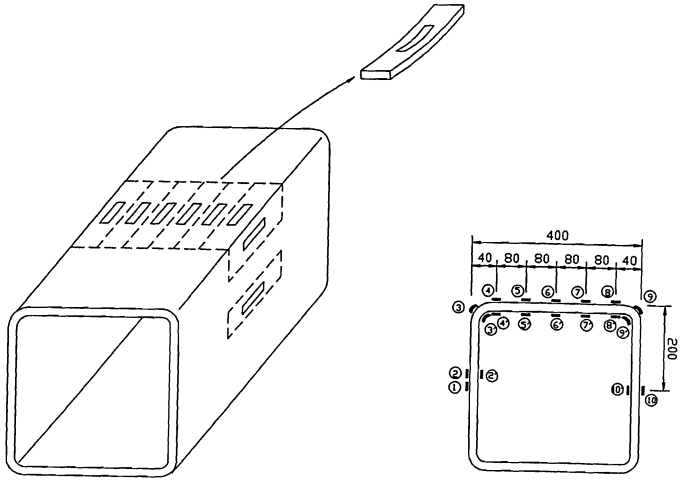

Fig. 2 Sectioning Technique and Strain Gauge Location

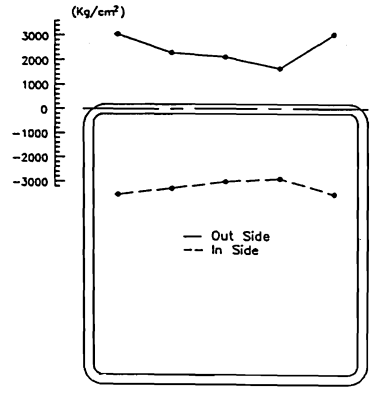

(1 kg/cm^2 = 0.098 MPa)

Fig. 3 Residual Stress Distribution (SHS 400mm×400mm×12mm Column)

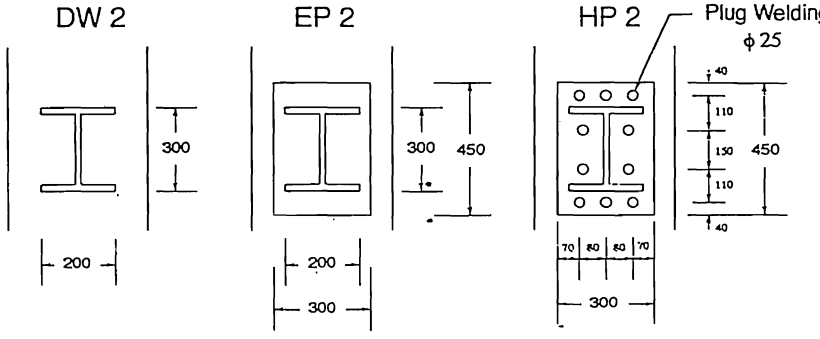

Fig. 4 Geometry of Three Connection Types

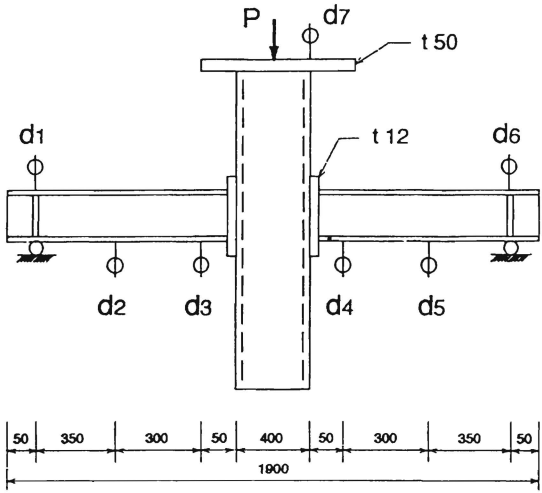

Fig. 5 Beam-Column Connection Test Configuration

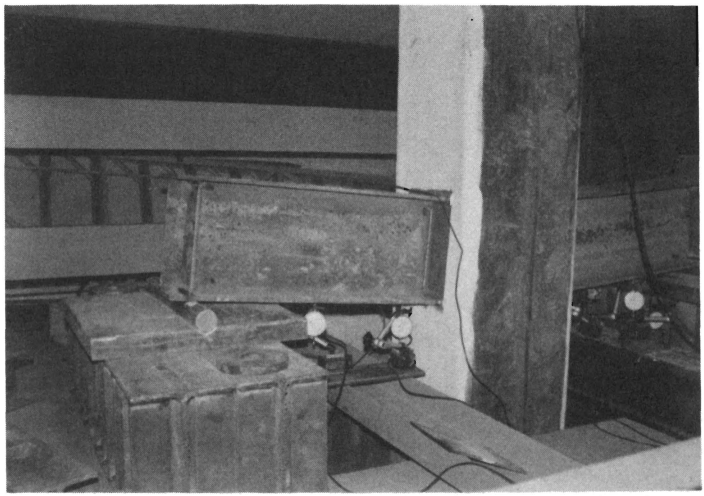

Fig. 6 Failure Mode of Beam-Column Connections

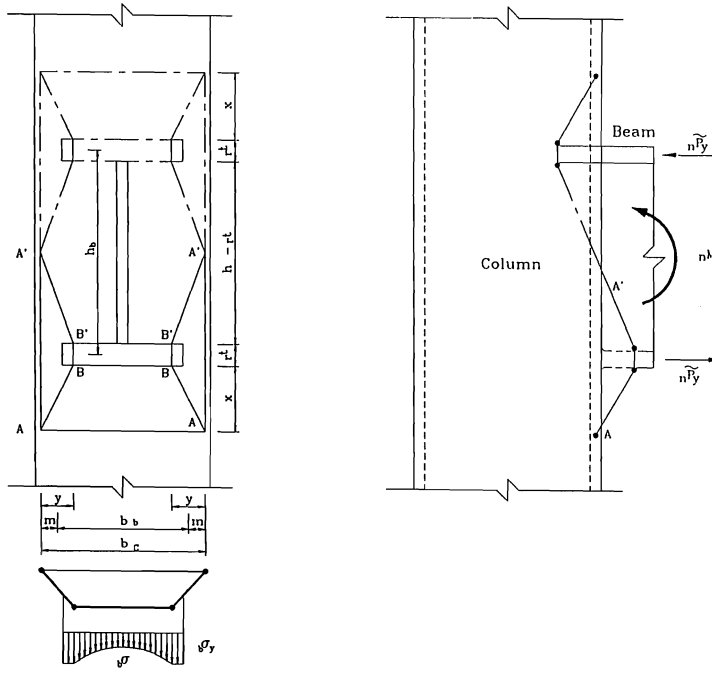

Fig. 7a Yield Line Model (DW Type)

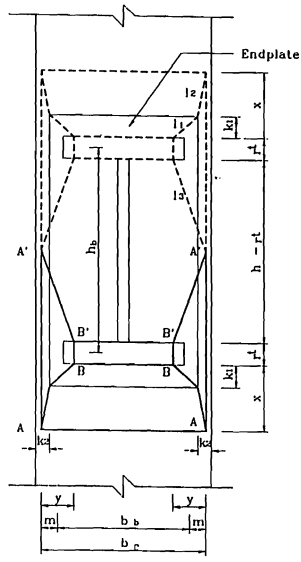

Fig. 7b Yield Line Model (EP Type)

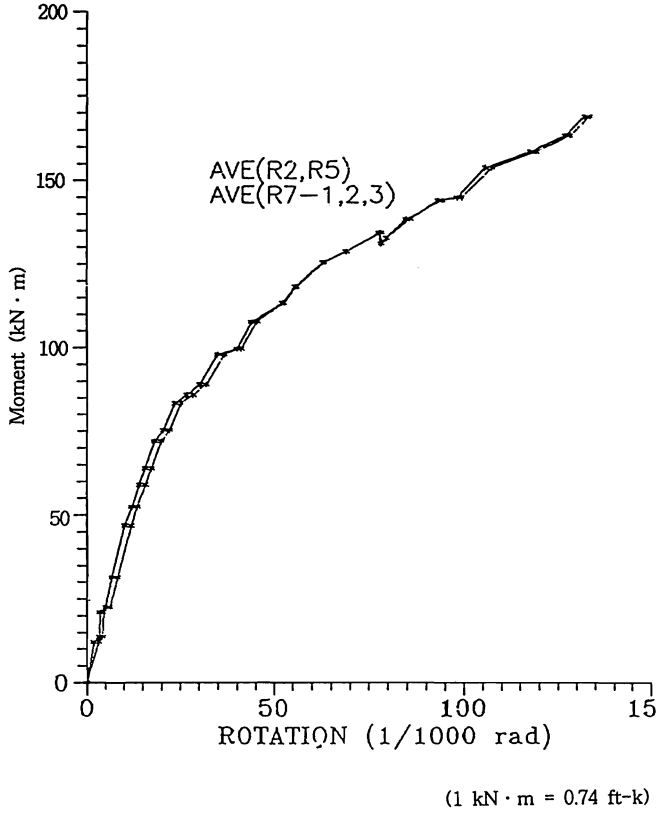

Fig. 8 Moment-Rotation Curves of the Test Connections (EP 2)

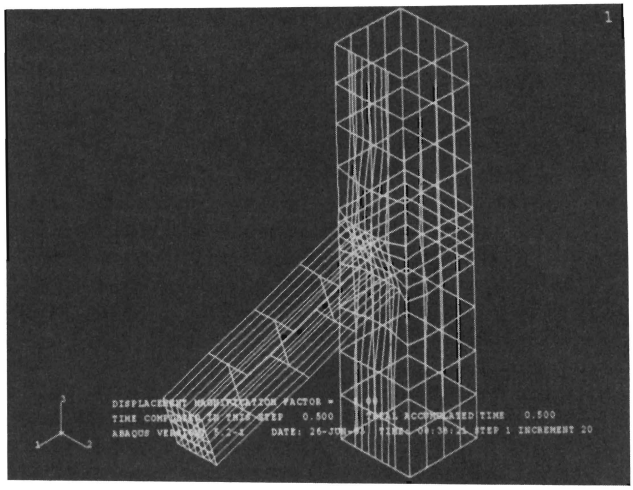

Fig. 9 Typical Deformed Mode of Connection

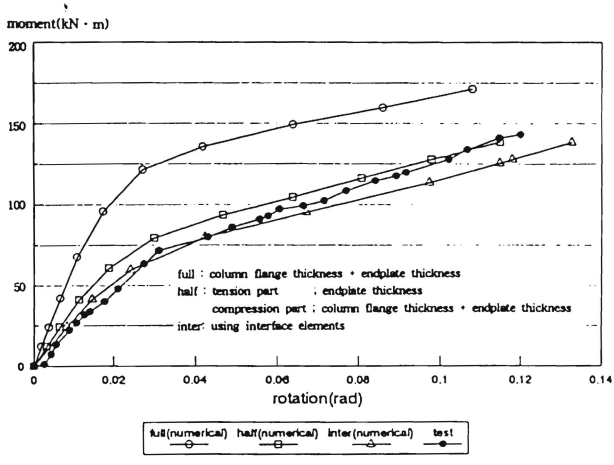

(1kN · m = 0.74 ft-k)

Fig. 10 Moment-Rotation Curves (EP 2)

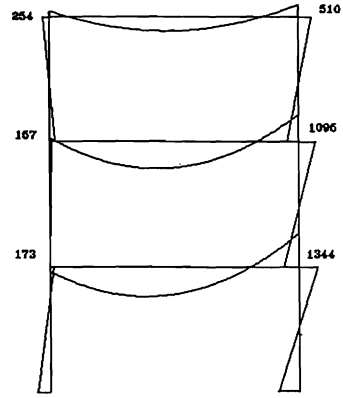

Fig. 11a Moment Distribution of Semi-Rigid Frame

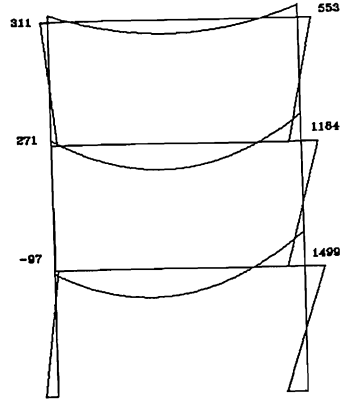

Fig. 11b Moment Distribution of Rigid Frame